**Joint ERCOFTAC/EU-CTFF**
**European Drag Reduction and Flow Control Meeting – EDRFCM 2022**
**September 6th–9th, 2022, Paris, France**

# NUMERICAL INVESTIGATION OF HOMOGENEOUS BLOWING AND SUCTION ON AN AIRFOIL IN COMPRESSIBLE FLOW

**A. Frede, A. Stroh, G. Fahland, D. Gatti**
Institute of Fluid Mechanics, Karlsruhe Institute of Technology, 76131 Karlsruhe, Germany

## INTRODUCTION

Commercial air traffic is responsible for about 2.6 % of the global carbon dioxide emissions, with an annual increase of 5.3 % in the passenger-kilometers, the contribution of $CO_2$ emissions from air traffic to the global emission will rise in the next years [2]. Among the means to reduce $CO_2$ emissions by improving the efficiency of an aircraft, the reduction of friction drag in turbulent boundary layers is promising despite the technological challenges and is considered here. Passive drag reduction strategies, like riblets, do not require additional energy and lead to a decrease in drag of about 6 % [5]. Active control strategies do require additional energy during the operation process, but promise to achieve larger viscous drag reduction margins.

Many studies show the effectiveness of uniform blowing and suction, an active control strategy (see, for instance, [3, 4, 1]). Considering canonical geometries, Kametani et al. [3] showed that uniform blowing reduced the skin friction drag and uniform suction increased it, while Stroh et al. [4] investigated a drag-reduction control scheme by inducing a constant mass flux in wall-normal direction, with a positive effect on the drag. Fahland et al. [1] conducted a large parametric study about homogeneous wall-normal blowing and suction on airfoils. Incompressible RANS simulations were conducted with a NACA4412 profile. The most promising configuration was found to be blowing on the pressure side, where the effect of drag reduction increases with increasing Reynolds number ($Re$). A positive effect on the aerodynamic efficiency was also found with suction on the suction side. Blowing on the suction side does not show a global benefit, a reduction in the friction drag can be observed, accompanied by a large increase in the pressure drag, so overall a decrease in the aerodynamic efficiency.

However, for commercial aviation bodies with a complex geometry as well as compressible flows are relevant. In this study the effect of compressibility, i.e. of the Mach number $Ma$, on the performance of wall-normal blowing and suction is investigated.

## METHODOLOGY

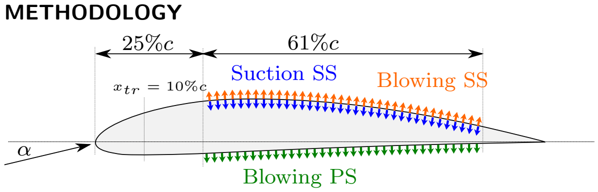


Figure 1: Sketch NACA4412 with the three different control regimes [1].

The compressible flow around different airfoils of chord length $c$ is investigated with RANS simulations, which are conducted with the steady-state solver included in the open-source CFD code $SU^2$. The $k$-$\omega$-SST model was used as the turbulence model. The transition was fixed at $x/c = 0.1$.

The applied control strategy is homogeneous wall-normal blowing and suction. The control region on the airfoil is fixed between $x/c = 0.25\,\%$ and $x/c = 0.86\,\%$. Three control configuration were investigated: blowing on the suction side, suction on the suction side and blowing on the pressure side. For the parametric study different parameters such as the Reynolds number, the Mach number, the airfoil shape, angle of attack (AoA) and control intensity were varied. Figure 1 shows a sketch of a NACA4412 with the different control regions.

## RESULTS FOR NACA4412

The drag polar for a variation of the AoA between $\alpha = -2°$ and $8°$ for a NACA4412 is shown in Figure 2. The chord Reynolds number was fixed at $Re = cu_\infty/\nu = 1 \cdot 10^6$, where $u_\infty$ is the freestream velocity. The freestream Mach number is $Ma = u_\infty/a_\infty = 0.4$, where $a_\infty$ is speed of sound at freestream, and the control intensity was $v_{blc} = 0.1\,\%\,u_\infty$ and $0.2\,\%\,u_\infty$.

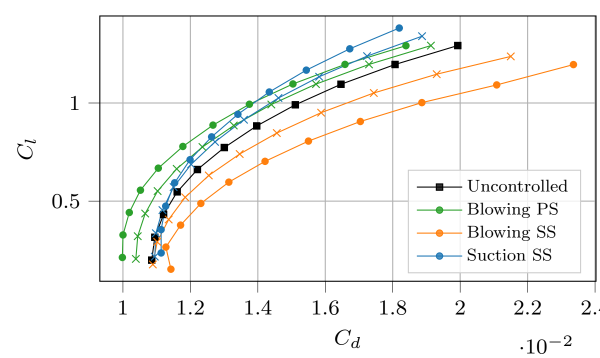


Figure 2: Polar plot of an example case for $Re = 1 \cdot 10^6$, $Ma = 0.4$ and $v_{blc} = 0.1\,\%\,u_\infty$ (× symbols) and $v_{blc} = 0.2\,\%\,u_\infty$ (● symbols).

For blowing on the suction side an overall increase in the drag coefficient $C_d = \frac{2D'}{\varrho_\infty u_\infty^2 c}$ ($D'$ is the drag per unit depth and $\varrho_\infty$ the freestream density) can be observed, which is accompanied by a decrease in the lift coefficient, $C_l = \frac{2L'}{\varrho_\infty u_\infty^2 c}$ ($L'$ is the lift force per unit depth). The effect is smaller at lower AoA, but significant at higher AoA. The boundary layer thickness is increased, which is accompanied by a decrease in the friction coefficient $C_f = \frac{2\tau_w}{\varrho_\infty u_\infty^2}$ ($\tau_w$ is the wall shear stress), but also a large increase in the pressure drag $C_p = \frac{2(p-p_\infty)}{\varrho_\infty u_\infty^2}$ ($p$ and $p_\infty$ are the local and freestream pressure). The increase in the pressure coefficient can be observed in Figure 3. The separation of the boundary layer is moved upstream, which can be observed in the wall shear stress curve (Figure 3) crossing zero at lower x-values compared to the uncontrolled case.

Opposite effects can be observed for suction on the suction side. The lift increases compared to the uncontrolled case, which is particularly significant for high AoA. A reduction of the drag can be observed for higher AoA. Suction leads to an increase in the wall shear stress, which can be observed in Figure 3, but also to a reduction of the pressure drag. This is accompanied by a reduction of the pressure coefficient for almost the whole suction side (Figure 3). For $\alpha = 5°$ the lift increases by about 6.6 % and the drag decreases by about 5.1 % for $v_{blc} = 0.2\,\%\,u_\infty$.

The pressure gradient on the pressure side is mild compared to the pressure gradient on the suction side (Figure 3). Blowing on this side reduces the friction drag, but the boundary layer does not increase significantly. So an overall decrease in the drag can be observed, as of about 9 % for $v_{blc} = 0.2\,\%\,u_\infty$. The lift is not affected by blowing on the pressure side.

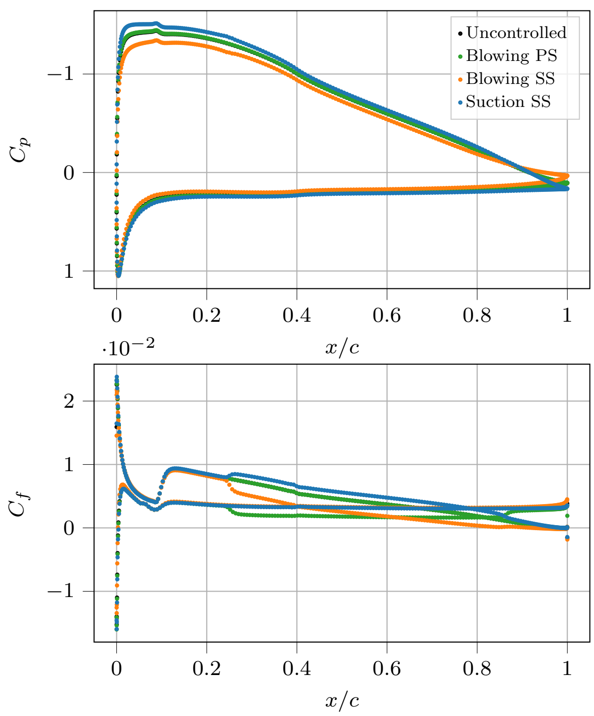


Figure 3: Pressure coefficient $C_p$ and skin friction coefficient $C_f$ for $Re = 1 \cdot 10^6$, $Ma = 0.4$, NACA4412, $\alpha = 5°$ and $v_{blc} = 0.2\,\%\,u_\infty$.

## RESULTS FOR RAE2822

For the transonic flow the RAE2822 airfoil was investigated. As an example case the results for $Re = 1 \cdot 10^6$, $Ma = 0.8$, $AoA = 1°$ and $v_{blc} = 0.2\,\%\,u_\infty$ are shown in Figures 4.

In this configuration the effect of the homogeneous wall-normal blowing and suction on the position of the shock is investigated. As already observed for the NACA4412 airfoil suction on the suction side leads to an increase in the skin friction coefficient on the suction side and blowing leads to a reduction of the skin friction coefficient on the respective side. Suction on the suction side leads to a shift of the shock position further downstream on the airfoil's surface, respectively blowing on the suction side shifts the shock further upstream. The same can be observed for the pressure side, where blowing also leads to a shift of the shock position further upstream. Further simulations with lower Mach numbers will be conducted, to investigate the effect of the active control strategy on the shock position at the suction side.

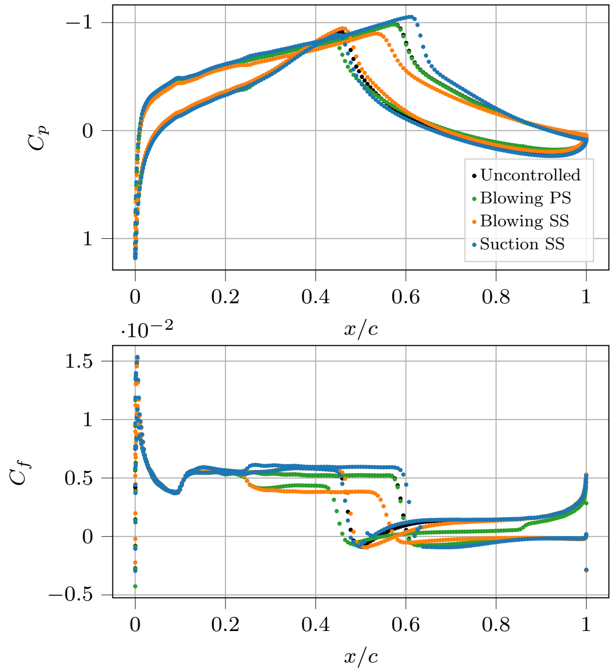


Figure 4: Pressure coefficient $C_p$ and skin friction coefficient $C_f$ for $Re = 1 \cdot 10^6$, $Ma = 0.8$, RAE2822, $\alpha = 1°$ and $v_{blc} = 0.2\,\%\,u_\infty$.

## CONCLUSION

The first results of the parametric study show promising results, that homogeneous wall-normal blowing and suction has a positive effect on the aerodynamic efficiency. The two most promising control configurations in the compressible flow for a NACA4412 airfoil are blowing on the pressure side and suction on the suction side, which agrees with previous studies in the incompressible regime. In the transonic regime the control strategy also influences the position of the shock. In future studies this effect should be investigated in more detail, by a detailed variation of the position and the size of the control regime as well as different control intensities to see the effect on the shock position.

## REFERENCES


[1] G. Fahland, A. Stroh, B. Frohnapfel, M. Atzori, R. Vinuesa, P. Schlatter, and D. Gatti. *AIAA Journal*, 59(11):4422–4436, 2021.

[2] International Energy Agency (IEA). Energy technology perspectives 2016, 2016.

[3] Y. Kametani and K. Fukagata. *J. Fluid Mech.*, 681:154–172, August 2011.

[4] A. Stroh, Y. Hasegawa, P. Schlatter, and B. Frohnapfel. *J. Fluid Mech.*, 805:303–321, October 2016.

[5] M. J. Walsh, W. L. Sellers, and C. B. McGinley. *Journal of Aircraft*, 26(6):570–575, 1989.